DRAFT VERSION OCTOBER 24, 2024
Typeset using LaTeX **twocolumn** style in AASTeX631

Ground-based light curve follow-up validation observations of TESS object of interest TOI-5907

EVAN PAPPS[1] AND PETER PLAVCHAN[1]

[1]*Department of Physics and Astronomy, 4400 University Drive MS 3F3, George Mason University, Fairfax, VA 22030, USA*

(Dated: 19 August 2024)

1. ABSTRACT

We present the findings of ground-based light curve follow-up validation observations of TESS object of interest TOI-5907. The TESS mission only captured a transit in one sector, making TOI-5907 a prime target for additional observations. Following time-series observations during a predicted transit using GMU's 0.8 m Ritchey-Chretien on 20 June 2024 and 28 June 2024, the images were reduced, plate solved, and aligned using AstroImageJ to generate a light curve. This light curve was supplemented with TESS data and fitted using EXOFASTv2 to generate updated values for the system. While the NEB check was unable to rule out the possibility of an eclipsing binary in this instance, a transit was detected on the 20th. This allowed for an updated period and transit duration, which will be valuable for future observations.

2. INTRODUCTION

The Transiting Exoplanet Survey Satellite (TESS) mission began observing nearly the entire sky in July of 2018. At the time of writing, TESS has identified 7204 TESS Object of Interests (TOIs). Of those, 4646 remain unconfirmed, 542 have been confirmed, and 2016 were determined to be false positives.[1] The follow-up work done to verify the remaining TESS candidates is difficult, but essential to achieving the purpose of the mission. That is continue to improve the classification of the qualities of the planets and identify any forms of false positives.

Released in 2019, the public exoplanet fitting software EXOFASTv2 is an improvement on the original 2013 version. It is capable of fitting a number of different data types and providing a publication-quality figures and a table of all output parameters.[2] The program utilizes the Markov chain Monte Carlo (MCMC) algorithm to draw samples from a probability distribution. It explores a series of values for the system simultaneously evaluates the fit and corrects for the next step. It will be utilized to process both TESS and ground-based data and generate associated values TOI-5907 and its host star.

TOI-5907 is predicted by ExoFOP to be a 'Hot Jupiter', with a radius $8.31454 \pm 2.06084\ R_{\oplus}$ and a brief period of 0.6583175 ± 0.0000797 days. This makes TOI-5907 a fairly standard TESS planet, among the many of its kind. It orbits a Sun-like star with a radius $1.08017 \pm 0.0546734\ R_{\odot}$.

In the following manuscript, we outline the observations and methods used to gather and process the data in an effort to classify the candidate. We also describe the difficulties of Ground-based follow-up validation of less recent TESS observations, including transit timing decay. Transit timing decay is the problem of increasing uncertainty as to when a transit will occur the longer the time period from the most recent observation. TOI-5907 was originally identified as a planet candidate by TESS on 10 November 2022. Since its observation, it has received little attention. This makes TOI-5907 a prime candidate for strengthening the transit timing certainty, but also causes timing observations to be more difficult.

3. OBSERVATIONS

In Section 3.1 we present the TOI-5907 and its exoplanet candidate properties, as well as its host star properties from the TESS Input Catalog. In Section 3.2 we present the TESS sector light curve and SED. In Section 3.3, we present a summary of the observational data collected with the George Mason University 0.8m telescope.

3.1. *System Properties and Priors*

Below are the predicted values for the system as published by the Exoplanet Follow Up (ExoFOP) Research Team. These will be inputted as the starting values for the EXOFASTv2 program. TOI-5907 orbits its Sun-like star with a brief period of 0.6583175 days. The value of 0.26009 for the extinction of the target can be found on the NASA/IPAC In-

[1] NASA. (2024). Exoplanet and Candidate Statistics. Caltech.edu. https://exoplanetarchive.ipac.caltech.edu/docs/counts_detail.html

[2] Eastman, J. D., Rodriguez, J. E., Agol, E., Stassun, Keivan G, Beatty, T. G., Vanderburg, A., Scott, G. B., Collins, K. A., & Luger, R. (2019). EXOFASTv2: A public, generalized, publication-quality exoplanet modeling code. ArXiv.org. https://arxiv.org/abs/1907.09480

frared Science Archive.[3] The tc included in the table is for the TESS observation.

Parameter	Value
$R_*(R_\odot)$	1.08017
$M_*(M_\odot)$	1.03
$T_{eff}(K)$	5766
parallax (mas)	4.786
$[Fe/H]$	0.107
Extinction	0.26009
Period (days)	0.6583175
tc (JDM)	2459823.85046

Table 1. Priors used in EXOFASTv2.[a]

[a] Bieryla, A., & ExoFOP Team. (2015). ExoFOP TIC 387318486. Caltech.edu. https://exofop.ipac.caltech.edu/tess/target.php?id=387318486

3.2. *TESS Sector Light Curve and SED Data*

TESS observed the target in Sector 55. The transit data can be downloaded from the ExoFOP database using the corresponding TIC number.[4] As well, ExoFOP presents a table of stellar magnitudes. The SED bands that were utilized in the fit are presented in the table below. A list of accepted SED bands for EXOFASTv2 can be found on the GitHub.[5]

Band	Value	Error
BT	13.729	0.014
VT	12.95	0.126
J2M	11.797	0.027
H2M	11.481	0.034
K2M	11.413	0.024
WISE1	11.356	0.023
WISE2	11.356	0.021
WISE3	11.128	0.134

Table 2. SED Data used in EXOFASTv2.[a]

[a] Bieryla, A., & ExoFOP Team. (2015). ExoFOP TIC 387318486. Caltech.edu. https://exofop.ipac.caltech.edu/tess/target.php?id=387318486

3.3. *Ground-Based Follow-Up*

We observed TOI-5907 on 20 June 2024 and 28 June 2024 at George Mason University in Fairfax, USA. Both observations utilized the 0.8 m Ritchey-Chretien and were taken in using the R filter. The observations spanned from 22:55-04:30 EDT and 22:25-04:35 EDT, respectively. An example image of the field of view is provided below.

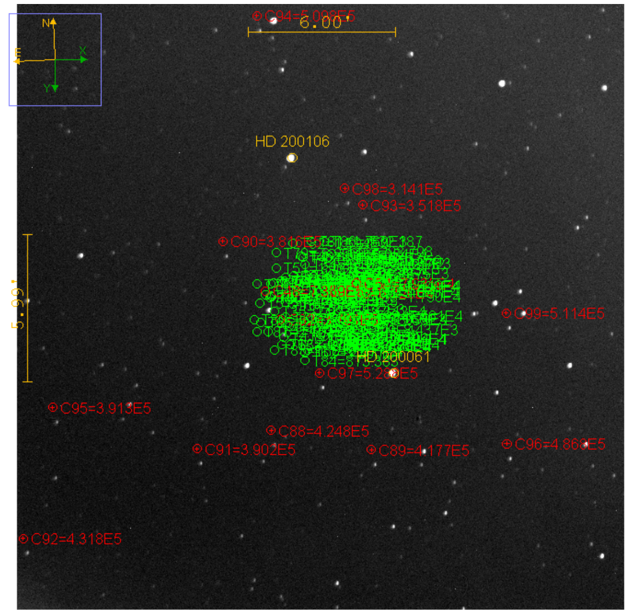

Figure 1. 6' field of view from the 0.8 m Ritchey-Chretien on 2024/06/20.

The observation on the 20th consisted of 205 exposures for 85s each, and the observation on the 28th consisted of 172 exposures for 90s each. Unfortunately, on the 20th there were 23 bad images found throughout the image stack, resulting in 182 usable images. While this is not an uncommon number of bad images, the remaining data, particularly in the first half of the night, had a significant amount of noise. Moreover, on the 28th there were 97 consecutive bad images. This left only the 75 earliest images in the night. While the remaining images had a low amount of noise, they likely do not contain a transit as discussed in the Analysis.

4. ANALYSIS

In Section 4.1, we present our analysis of the ground-based light curve using AstroImageJ. In Section 4.2 we present our tools used to analyze the TESS sector light curve curve, processed ground-based light curve, and SED using ExoFASTv2.

4.1. *Processing the Ground-Based Light Curve*

AstroImageJ is the primary tool for preparing the ground-based light curve for EXOFASTv2.[6] Firstly, the images are

[3] IRSA. (n.d.). Galactic Dust Reddening and Extinction. NASA/IPAC Infrared Science Archive. https://irsa.ipac.caltech.edu/frontpage/

[4] Bieryla, A., & ExoFOP Team. (2015). ExoFOP TIC 387318486. Caltech.edu. https://exofop.ipac.caltech.edu/tess/target.php?id=387318486

[5] Eastman, J. (2022). Accepted SED Filter Names. GitHub. https://github.com/jdeast/EXOFASTv2/blob/master/sed/mist/filternames.txt

[6] Collins, K., Kielkopf, J., Stassun, K., & Hessman, F. (2017). AstroImageJ: Image processing and photometric extraction for ultra-precise astronomical light curves. The Astronomical Journal, 153(2), 77. https://doi.org/10.3847/1538-3881/153/2/77

reduced. The dark and flat images are used to subtract most of the noise and background artifacts in the science images. The dark images are taken with the shutter of the camera closed to get rid of any thermal noise that stemmed from the CCD sensor. The flat images are taken with the shutter completely open to get rid of any artificial noise by correcting any defective pixels and vignetting. The dark and flat images are stacked before being applied to the science images, all within AstroImageJ.

Plate solving each image assigns a value for Right Ascension and Declination to every pixel. This is essential to identifying and tracking stars in the image. It is done using Nova Astrometry through AstroImageJ.[7] After the plate solving is complete, images with large movements and failed plate solving are removed from the data set. The images are also aligned within the AstroImageJ application.

To produce a light curve with a measurements table, aperture photometry must be performed first. Aperture photometry is the process of subtracting the average local background light from the light of the target. This is done for many comparison stars as well, which can then be used as a standard to compare the target to in order to convert the instrumental magnitudes to standard magnitudes.[8]

Next, we attempt to eliminate the possibility that the TIC is a false positive, and is an eclipsing binary. This is known as the Near Eclipsing Binary (NEB) check. To do this, reference stars are imported to AstroImageJ from the Gaia Fields database.[9] Importing this data will allow the application to generate a dmag RMS plot, which will allow us to determine whether each star passes the NEB check.

Finally, the measurements table and light curve can be generated. This involves inputting parameters such as the predicted ingress/egress time, limb darkening coefficients, and basic stellar values. The fluxes of the target and reference star, as well as the detrending parameters, are selected to be plotted on the light curve. This will be covered in further detail along with the graph.

4.2. *Analysis in EXOFASTv2*

Both the TESS and GMU data can be used to fit the best values for the system in EXOFASTv2. To do this, multiple files must be prepared. The args file includes paths to the data files, and defines the length of the program run (set to 50000 steps in this case), the number of stars, and the number of planets. The priors file includes all of the starting values presented in Table 1. The SED file includes all of the magnitudes presented in Table 2. The data is ASCII plain text with the columns separated by spaces.

The table of measurements for the ground-based light curve produced in the previous section can now be fitted in EXOFASTv2. The formatting of transit files for the program is simple, and can be found in the documentation.[10] The BJD_{TBD}, $relfluxT1_n$, and $relfluxerrT1_n$ columns can be copied from the measurements table. Greater detail on extracting AstroImageJ light curves for input into EXOFASTv2 is outlined succinctly in an AstroImageJ forum blog post.[11] As with the SED file each value within a row is separated by spaces; an example is shown in the table below:

BJD_{TDB}	$relfluxT1_n$	$relfluxerrT1_n$
2460482.62254755	0.976582371297858	0.0007122341563821
2460482.62371083	0.98332939862344	0.0007073424875513
2460482.62487537	0.964014538560121	0.0006959201934261

Table 3. Example transit light curve file data.

The system is then left to run. The best fit results are presented in the following section.

5. RESULTS

We now present the results of ground-based observations and best fit modelling.

Figure 2 contains the light curve of UT2024-06-20. In blue is the normalized flux of T1, which is the raw brightness flux data plotted without any detrending. This flux does not fit the transit model without detrending due to systematic trends and external factors that cause the data to be diluted. In pink is the residuals of T1, which have error bars of each data point to show the uncertainty and accuracy of the points in comparison to the transit model. In black is a light curve of one of the reference stars for comparison. Finally, at the bottom of our light curve are the detrending parameters of Sky/Pixel_T1, Width_T1, AIRMASS, tot_C_cnts, X(FITS)_T1, and Y(FITS)_T1.

The dmag RMS plot in Figure 3 contains a scatter of the reference stars, as well as two lines. These lines indicate a border, below which any reference stars are likely cleared and definitively cleared for the NEB check.

[7] Astrometry.net. (n.d.). Nova.astrometry.net. https://nova.astrometry.net/

[8] Richmond, M. (n.d.). Simple Aperture Photometry by Hand. Spiff.rit.edu. http://spiff.rit.edu/classes/phys445/lectures/photom/photom.html

[9] Louisville University Department of Physics and Astronomy. (2016). Gaia Fields for TESS Follow-up. Louisville.edu. https://www.astro.louisville.edu/gaia_to_aij/

[10] Eastman, J. (2017, June 19). Accepted Transit File Formats in EXOFAST. Exoplanetarchive.ipac.caltech.edu. https://exoplanetarchive.ipac.caltech.edu/docs/exofast/transit_upload.html

[11] Collins, K. (2019). Output an AIJ Light Curve data subset for input to EXOFAST or other global modeling tools. http://astroimagej.170.s1.nabble.com/Output-an-AIJ-Light-Curve-data-subset-for-input-to-ExoFAST-or-other-global-modeling-tools-td1109.html

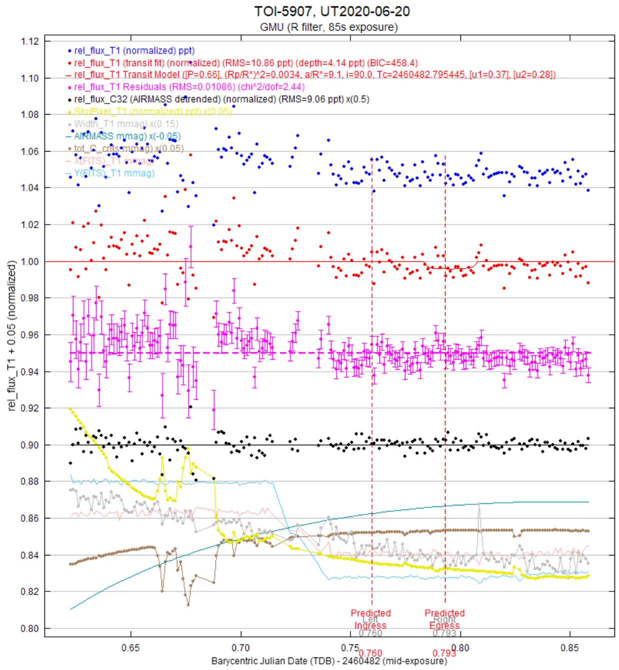

Figure 2. UT2020-06-20 Light curve and parameters.

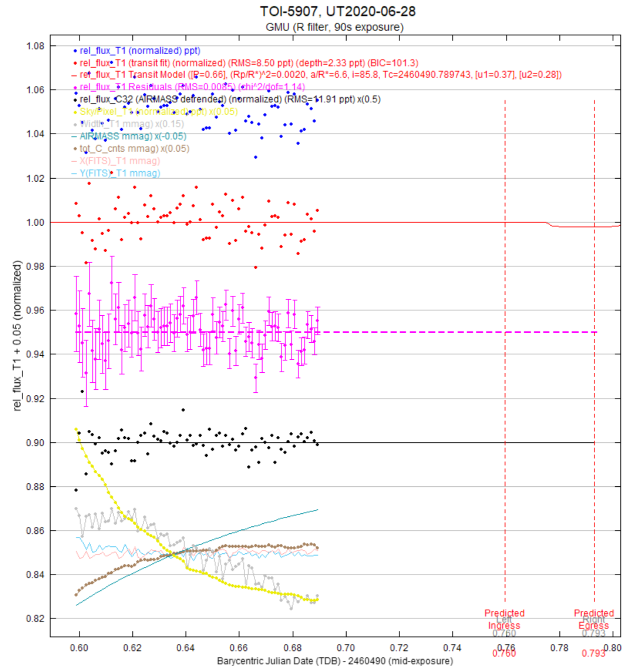

Figure 4. UT2020-06-28 Light curve and parameters.

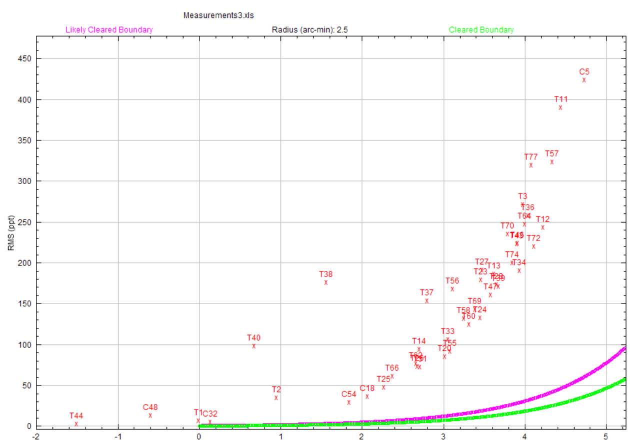

Figure 3. Dmag RMS plot used to perform the NEB check.

Figure 4 contains the light curve of UT2024-06-28. The same format applies as above.

Figure 5 contains the S55 TESS light curve and the ground-based observation on 2024-06-20. The black scatter is the measured flux, and the red line is the best fit for the transit as predicted by EXOFASTv2.

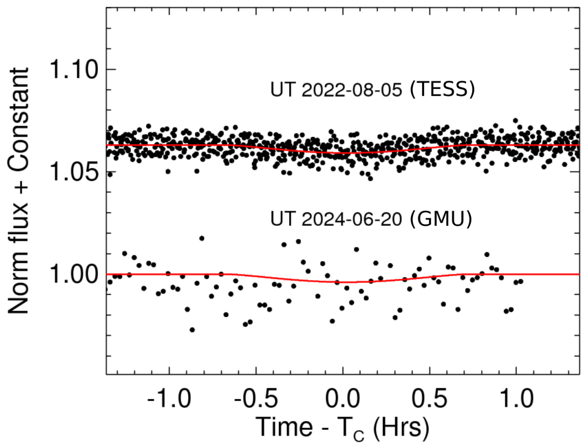

Figure 5. Transit light curve generated by EXOFASTv2 including TESS (top) and GMU (bottom).

Figure 6 contains the Spectral Energy Distribution of the star. The red error boxes are the measured magnitudes at their respective λ, and the black line is the best fit as predicted by EXOFASTv2.

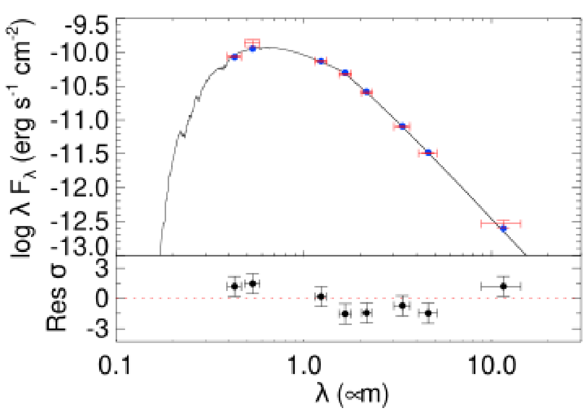

Figure 6. SED of host star generated by EXOFASTv2.

Finally, Table 4 presents the best fit values for the host star (0) and the planet (b).

Table 4. Median values and 68% confidence interval for 387318486.1.

Parameter	Description	Values
Stellar Parameters:		0
M_*	Mass ($M_\odot$)	$0.908^{+0.082}_{-0.042}$
R_*	Radius ($R_\odot$)	1.03 ± 0.12
$R_{*,SED}$	Radius[1] ($R_\odot$)	$1.03^{+0.12}_{-0.14}$
L_*	Luminosity ($L_\odot$)	$1.06^{+0.28}_{-0.23}$
F_{Bol}	Bolometric Flux (cgs)	$7.8^{+2.0}_{-1.7} \times 10^{-10}$
ρ_*	Density (cgs)	$1.19^{+0.51}_{-0.30}$
$\log g$	Surface gravity (cgs)	$4.379^{+0.098}_{-0.083}$
$T_{\rm eff}$	Effective temperature (K)	5777^{+79}_{-57}
$T_{\rm eff,SED}$	Effective temperature[1] (K)	5790 ± 130
[Fe/H]	Metallicity (dex)	$-0.19^{+0.27}_{-0.23}$
$[{\rm Fe/H}]_0$	Initial Metallicity[2]	$-0.13^{+0.24}_{-0.21}$
Age	Age (Gyr)	$8.1^{+2.9}_{-3.6}$
EEP	Equal Evolutionary Phase[3]	392^{+28}_{-43}
A_V	V-band extinction (mag)	$0.146^{+0.088}_{-0.099}$
σ_{SED}	SED photometry error scaling	64^{+18}_{-16}
ϖ	Parallax (mas)	$4.781^{+0.028}_{-0.026}$
d	Distance (pc)	$209.1^{+1.1}_{-1.2}$
Planetary Parameters:		b
P	Period (days)	$0.6583081^{+0.0000098}_{-0.0000091}$
R_P	Radius ($R_{\rm J}$)	$1.00^{+0.10}_{-0.13}$
M_P	Mass[4] ($M_{\rm J}$)	$1.08^{+0.62}_{-0.42}$
T_C	Time of conjunction[5] ($\rm BJD_{TDB}$)	$2460139.8376^{+0.0077}_{-0.0072}$
T_T	Time of min proj sep[6] ($\rm BJD_{TDB}$)	$2460139.8373^{+0.0049}_{-0.0050}$
T_0	Optimal conj time[7] ($\rm BJD_{TDB}$)	$2459798.1756^{+0.0058}_{-0.0057}$
a	Semi-major axis (AU)	$0.01456^{+0.00042}_{-0.00025}$
i	Inclination (Degrees)	$75.7^{+2.8}_{-4.2}$
e	Eccentricity	$0.49^{+0.12}_{-0.21}$
ω_*	Arg of periastron (Degrees)	-85^{+43}_{-34}
$T_{\rm eq}$	Equilibrium temp[8] (K)	2340^{+120}_{-140}
$\tau_{\rm circ}$	Tidal circ timescale (Gyr)	$0.0013^{+0.0089}_{-0.0011}$
K	RV semi-amplitude[4] (m/s)	12700^{+6100}_{-8800}
R_P/R_*	Radius of planet in stellar radii	$0.101^{+0.016}_{-0.020}$
a/R_*	Semi-major axis in stellar radii	$3.06^{+0.39}_{-0.29}$
δ	$\left(R_P/R_*\right)^2$	$0.0102^{+0.0035}_{-0.0036}$
$\delta_{\rm TESS}$	Transit depth in TESS (frac)	$0.00400^{+0.00052}_{-0.00058}$
τ	In/egress transit duration (days)	$0.0248^{+0.0032}_{-0.0041}$

Table 4 *continued*

Table 4 *(continued)*

Parameter	Description	Values	
T_{14}	Total transit duration (days)	$0.0497^{+0.0063}_{-0.0053}$	
T_{FWHM}	FWHM transit duration (days)	$0.0255^{+0.0037}_{-0.0029}$	
b	Transit impact parameter	$0.996^{+0.025}_{-0.043}$	
b_S	Eclipse impact parameter	$0.41^{+0.31}_{-0.13}$	
τ_S	In/egress eclipse duration (days)	$0.0050^{+0.0026}_{-0.0011}$	
$T_{S,14}$	Total eclipse duration (days)	$0.0432^{+0.0097}_{-0.0098}$	
$T_{S,FWHM}$	FWHM eclipse duration (days)	$0.0377^{+0.0083}_{-0.0096}$	
$\delta_{S,2.5\mu m}$	BB eclipse depth at 2.5μm (ppm)	1610^{+390}_{-470}	
$\delta_{S,5.0\mu m}$	BB eclipse depth at 5.0μm (ppm)	2700^{+710}_{-830}	
$\delta_{S,7.5\mu m}$	BB eclipse depth at 7.5μm (ppm)	3140^{+850}_{-980}	
ρ_P	Density[4] (cgs)	58^{+52}_{-44}	
$logg_P$	Surface gravity[4] (cgs)	$5.07^{+0.25}_{-0.58}$	
Θ	Safronov Number	$1.52^{+0.99}_{-1.1}$	
$\langle F \rangle$	Incident Flux (10^9 erg s^{-1} cm^{-2})	$5.5^{+1.9}_{-1.5}$	
T_P	Time of Periastron (BJD_{TDB})	$2460139.67^{+0.35}_{-0.15}$	
T_S	Time of eclipse (BJD_{TDB})	2460139.52 ± 0.11	
T_A	Time of asc node (BJD_{TDB})	$2460139.616^{+0.098}_{-0.12}$	
T_D	Time of desc node (BJD_{TDB})	$2460140.076^{+0.11}_{-0.089}$	
V_c/V_e	Scaled velocity[9]	$1.50^{+0.33}_{-0.40}$	
$((1-R_P/R_*)^2-b^2)^{1/2}$	Transit chord	$0.474^{+0.044}_{-0.028}$	
$sign$		$1.43^{+0.38}_{-0.46}$	
$e\cos\omega_*$		0.02 ± 0.23	
$e\sin\omega_*$		$-0.41^{+0.27}_{-0.15}$	
$M_P \sin i$	Minimum mass[4] (M_J)	$1.02^{+0.56}_{-0.36}$	
M_P/M_*	Mass ratio[4]	$0.0011^{+0.00062}_{-0.00042}$	
d/R_*	Separation at mid transit	$4.0^{+1.0}_{-1.1}$	
P_T	A priori non-grazing transit prob	$0.224^{+0.092}_{-0.049}$	
$P_{T,G}$	A priori transit prob	$0.274^{+0.095}_{-0.054}$	
P_S	A priori non-grazing eclipse prob	$0.53^{+0.13}_{-0.14}$	
$P_{S,G}$	A priori eclipse prob	0.65 ± 0.17	
Wavelength Parameters:		TESS	
u_1	Linear limb-darkening coeff	$0.293^{+0.045}_{-0.041}$	
u_2	Quadratic limb-darkening coeff	$0.282^{+0.038}_{-0.041}$	
Transit Parameters:		TESS UT 2022-08-05 (TESS)	TESS UT 2024-06-20 (TESS)
σ^2	Added Variance	$1.281^{+0.047}_{-0.050} \times 10^{-5}$	$0.000143^{+0.000017}_{-0.000014}$
F_0	Baseline flux	$1.000095^{+0.000077}_{-0.000082}$	$0.96993^{+0.00095}_{-0.00091}$

Table 4 *continued*

Table 4 *(continued)*

Parameter	Description	Values

See Table 3 in(Eastman, 2019) for a detailed description of all parameters[12]

[1] This value ignores the systematic error and is for reference only

[2] The metallicity of the star at birth

[3] Corresponds to static points in a star's evolutionary history. See §2 in (Dotter, 2016).[13]

[4] Uses measured radius and estimated mass from (Chen & Kipping, 2017)[14]

[5] Time of conjunction is commonly reported as the "transit time"

[6] Time of minimum projected separation is a more correct "transit time"

[7] At the epoch that minimizes the covariance between T_C and Period

[8] Assumes no albedo and perfect redistribution

6. DISCUSSION

We now present our interpretation of the results. In Section 6.1 we discuss the ground-based light curves and the target's confirmation. In Section 6.2 we place the results of the EXOFASTv2 model in the context of the greater field of follow-up of candidate exoplanets from the NASA TESS mission and target's identification.

6.1. *Target Confirmation*

Firstly, let us discuss the first observation on 2024-06-20. There is a high level of noise in the first half of the observations, but fortunately the predicted transit is located later. The NEB check revealed an inconclusive result, with no cleared reference stars. The second observation on 2024-06-28 was even less successful. While there were images with a high level of noise, the second half of the observation was subject to excessive streaking. Due to the predicted transit being located during this time, the data could not aid in the NEB check, and was not used in the EXOFASTv2 model.

6.2. *Target Identification*

The ground-based light curve yielded similar results to that of the TESS data. The transit depth and duration were similar, which aided in updating the event timing. The period produced by EXOFASTv2 is $0.6583081^{+0.0000098}_{-0.0000091}$ days. The star is Sun-like in mass, radius, and temperature. Given the estimated stellar age of $8.1^{+2.9}_{-3.6}$ Gyr, the star is in the latter half of its main-stage sequence. With a R_J of $1.00^{+0.10}_{-0.13}$, M_J of $1.08^{+0.62}_{-0.42}$, and Equilibrium Temperature of 2340^{+120}_{-140} K, TOI-5907 is likely a Hot Jupiter. When the orbit of Hot Jupiters becomes very elliptical, they go through a process called Tidal migration. The orbit gradually becomes circular due, due to the gravitational bulge induced by the solar tides creating torque, causing the semi-major axis to decrease.[15] The high eccentricity of $0.49^{+0.12}_{-0.21}$ may mean that Tidal migration is incomplete given its close proximity to the star.

7. CONCLUSIONS AND FUTURE WORK

TOI-5907 was unable to be confirmed by the two ground-based light curve observations, however the data was used alongside public TESS data to produce new values for the system. The model agrees with a Hot Jupiter orbiting a Sun-like star.

Unfortunately, due to the processing power of the dedicated computer and the time constraints, the program was only run for 50000 steps. This brevity can lead to significant errors as the program may not have been given sufficient time to explore all possible values. Therefore, it is recommended that the program be run for significantly longer to allow for more significant conclusions to be made about the system.

Further observations with TESS and ground-based telescopes will aid in strengthening the certainty of any predictions made about the PC. Radial velocity measurements would aid in determining the mass and density of the target, and where it falls on the threshold of the Hot Jupiter classification.

[15] Fortney, J., Dawson, R., & Komacek, T. (2021). Hot Jupiters: Origins, Structure, Atmospheres. Journal of Geophysical Research: Planets, 126(3). https://doi.org/10.1029/2020je006629

8. ACKNOWLEDGEMENTS

We would like to gratefully acknowledge the support of the Department of Physics and Astronomy at George Mason University, wherein this research was carried out.

This research has made use of the Exoplanet Follow-up Observation Program website, which is operated by the California Institute of Technology, under contract with the National Aeronautics and Space Administration under the Exoplanet Exploration Program.

This research has made use of the NASA/IPAC Infrared Science Archive, which is funded by the National Aeronautics and Space Administration and operated by the California Institute of Technology.

9. REFERENCES

Astrometry.net. (n.d.). Nova.astrometry.net. https://nova.astrometry.net/

Bieryla, A., & ExoFOP Team. (2015). ExoFOP TIC 387318486. Caltech.edu. https://exofop.ipac.caltech.edu/tess/target.php?id=387318486

Chen, J., & Kipping, D. (2016). Probabilistic forecasting of the masses and radii of other worlds. The Astrophysical Journal, 834(1), 17. https://doi.org/10.3847/1538-4357/834/1/17

Collins, K., Kielkopf, J., Stassun, K., & Hessman, F. (2017). AstroImageJ: Image processing and photometric extraction for ultra-precise astronomical light curves. The Astronomical Journal, 153(2), 77. https://doi.org/10.3847/1538-3881/153/2/7

Dotter, A. (2016). MESA isochrones and stellar tracks (MIST) 0: Methods for the construction of stellar isochrones. The Astrophysical Journal Supplement Series, 222(1), 8. https://doi.org/10.3847/0067-0049/222/1/8

Eastman, J. (2022). Accepted SED Filter Names. GitHub. https://github.com/jdeast/EXOFASTv2/blob/master/sed/mist/filternames.txt

Eastman, J. D., Rodriguez, J. E., Agol, E., Stassun, Keivan G, Beatty, T. G., Vanderburg, A., Scott, G. B., Collins, K. A., & Luger, R. (2019). EXOFASTv2: A public, generalized, publication-quality exoplanet modeling code. ArXiv.org. https://arxiv.org/abs/1907.09480

Eastman, J. (2017, June 19). Accepted Transit File Formats in EXOFAST. Exoplanetarchive.ipac.caltech.edu.

https://exoplanetarchive.ipac.caltech.edu/docs/exofast/ transit_upload.html

Fortney, J., Dawson, R., & Komacek, T. (2021). Hot Jupiters: Origins, Structure, Atmospheres. Journal of Geophysical Research: Planets, 126(3). https://doi.org/10.1029/2020je006629

IRSA. (n.d.). Galactic Dust Reddening and Extinction. NASA/IPAC Infrared Science Archive. https://irsa.ipac.caltech.edu/frontpage/

Louisville University Department of Physics and Astronomy. (2016). Gaia Fields for TESS Follow-up. Louisville.edu. https://www.astro.louisville.edu/gaia_to_aij/

NASA. (2024). Exoplanet and Candidate Statistics. Caltech.edu. https://exoplanetarchive.ipac.caltech.edu/docs/counts_detail.html

Richmond, M. (n.d.). Simple Aperture Photometry by Hand. Spiff.rit.edu. http://spiff.rit.edu/classes/phys445/ lectures/photom/photom.html